Acta Biochim Biophys Sin 2024, 56(8): 1099–1107
https://doi.org/10.3724/abbs.2024110
Advance Access Publication Date: 28 June 2024
Original Article

Original Article

Glyco-signatures in patients with advanced lung cancer during anti-PD-1/PD-L1 immunotherapy

Xinyi Cao[1,2,†], Zhihuang Hu[3,4,†], Xiangying Sheng[5], Zhenyu Sun[1], Lijun Yang[5], Hong Shu[6], Xiaojing Liu[5], Guoquan Yan[1], Lei Zhang[1], Chao Liu[7], Ying Zhang[1,5,8], Huijie Wang[1,3,4,*], and Haojie Lu[1,5,8,*]

[1]Institutes of Biomedical Sciences and Shanghai Cancer Center, Fudan University, Shanghai 200032, China, [2]Department of Laboratory Medicine, Huashan Hospital, Fudan University, Shanghai 200040, China, [3]Department of Medical Oncology, Fudan University Shanghai Cancer Center, Shanghai 200032, China, [4]Department of Oncology, Shanghai Medical College, Fudan University, Shanghai 200032, China, [5]Department of Chemistry, Fudan University, Shanghai 200433, China, [6]Department of Clinical Laboratory, Guangxi Medical University Cancer Hospital, Nanning 530021, China, [7]Beijing Advanced Innovation Center for Precision Medicine, Beihang University, Beijing 100083, China, and [8]NHC Key Laboratory of Glycoconjugates Research, Fudan University, Shanghai 200032, China

[†]These authors contributed equally to this work.

*Correspondence address. Tel: +86-21-65675209; E-mail: wanghj98@hotmail.com (H.W.) / Tel: +86-21-54237618; E-mail: luhaojie@fudan.edu.cn (H.L.)

Received 23 January 2024 Accepted 25 March 2024

Abstract

Immune checkpoint inhibitors (ICIs) targeting programmed cell death 1/programmed cell death ligand-1 (PD-1/PD-L1) have significantly prolonged the survival of advanced/metastatic patients with lung cancer. However, only a small proportion of patients can benefit from ICIs, and clinical management of the treatment process remains challenging. Glycosylation has added a new dimension to advance our understanding of tumor immunity and immunotherapy. To systematically characterize anti-PD-1/PD-L1 immunotherapy-related changes in serum glycoproteins, a series of serum samples from 12 patients with metastatic lung squamous cell carcinoma (SCC) and lung adenocarcinoma (ADC), collected before and during ICIs treatment, are firstly analyzed with mass-spectrometry-based label-free quantification method. Second, a stratification analysis is performed among anti-PD-1/PD-L1 responders and non-responders, with serum levels of glycopeptides correlated with treatment response. In addition, in an independent validation cohort, a large-scale site-specific profiling strategy based on chemical labeling is employed to confirm the unusual characteristics of IgG N-glycosylation associated with anti-PD-1/PD-L1 treatment. Unbiased label-free quantitative glycoproteomics reveals serum levels' alterations related to anti-PD-1/PD-L1 treatment in 27 out of 337 quantified glycopeptides. The intact glycopeptide EEQFN^{177}STYR (H3N4) corresponding to IgG4 is significantly increased during anti-PD-1/PD-L1 treatment (FC = 2.65, $P = 0.0083$) and has the highest increase in anti-PD-1/PD-L1 responders (FC = 5.84, $P = 0.0190$). Quantitative glycoproteomics based on protein purification and chemical labeling confirms this observation. Furthermore, obvious associations between the two intact glycopeptides (EEQFN^{177}STYR (H3N4) of IgG4, EEQYN^{227}STFR (H3N4F1) of IgG3) and response to treatment are observed, which may play a guiding role in cancer immunotherapy. Our findings could benefit future clinical disease management.

Key words lung cancer, PD-1/PD-L1, immunotherapy, glycopeptide, IgG

Introduction

Lung cancer is one of the most common cancers and is considered as the leading cause of cancer-related mortality around the world [1]. Non-small cell lung cancer (NSCLC) accounts for more than 85% of lung cancers [2]. Only 25% of all patients with NSCLC survive more than 5 years after diagnosis, and only 6.9% of patients with advanced-stage NSCLC survive [3,4]. Immunotherapy has changed the current landscape of cancer treatment and shown

© The Author(s) 2024. This is an open access article distributed under the terms of the Creative Commons Attribution-NonCommercial-NoDerivs License (https://creativecommons.org/licenses/by-nc-nd/4.0/).

unparalleled improvement in survival rates [5]. Now, about one-third of cancer patients are eligible for the most widely used class of immunotherapy, immune checkpoint inhibitors (ICIs) [6]. PD-1 and its ligand PD-L1, are critical molecules in the immune checkpoint pathway [7].

However, immune checkpoint inhibitors can only benefit a minority of cancer patients. Anti-PD-1 antibodies produce an objective response in approximately one-quarter to one-fifth of patients with melanoma or renal cell cancer [8]. The response rate of single-agent PD-1/PD-L1 inhibitors in unselected NSCLC patients is 25% [9]. Considering the response limitations, the efficacy of anti-PD-1/PD-L1 immunotherapy has become the focus of current research [10]. In many solid tumors, novel immune features have been found in cancer patients who are more likely to benefit from immune-checkpoint inhibition, such as enhanced immune cell infiltration and $CD8^+$ T cell chemotaxis [11–13]. In melanoma, non-responders to anti-PD1 therapy exhibit the characteristics of a de-differentiated gene expression pattern [14]. Furthermore, the dynamic changes of intestinal microbiota have a highly significant linkage to the efficacy of PD-1 inhibitor treatment [15]. These available data indicate that the regulation of ICIs response is multifactorial and requires further study.

Glycosylation is one of the most important post-translational modifications of proteins, which is the key determinant of protein biological functions [16]. Most serum proteins are glycosylated, and some of the glycan alterations in serum are gaining more and more attention [17]. On the one hand, as a fundamental feature of proteins, glycosylation has a wide range of clinical implications in multidisciplinary fields, including oncology [18–20]. On the other hand, abnormal protein glycosylation amplifies the pathological signals, which is helpful for clinical judgment in patients with mild-to-no overt clinical symptoms [21–23]. In the past decade, a certain amount of methodologies and related software tools have greatly facilitated the analysis of glycan and glycopeptide quantification, especially N-glycopeptides, providing the possibility for widespread clinical application [24–26].

This study combined label-free and labeling glycoproteomic quantitative methods to discover and validate the changes in the serum glycoproteome attributable to ICIs treatment. Beyond the ongoing research, few studies have found systemic alterations in serum glycoproteome related to ICIs treatment. We aimed to understand the relationship between ICIs treatment and serum glycoproteins, and to seed unique and previously unexplored ideas for understanding the principle of immunotherapy in advanced lung carcinoma.

Materials and Methods

Study population

Twenty-seven serum specimens were obtained from the Department of Oncology at Shanghai Medical College, including 11 from patients with squamous cell carcinoma (SCC) and 16 from patients with adenocarcinoma (ADC). All clinical diagnoses were pathohistologically confirmed [27]. Information on demographics, diagnosis and staging, treatment, and treatment response was extracted from medical records and anonymized before analysis. Informed consent for the research was obtained from all patients. The acquisition and use of these specimens were approved by the Medical Ethics Committee of Fudan University Shanghai Cancer Center (approval no. 050432-4-1805C).

Criteria for response to treatment

The response to treatment was first evaluated at the date of treatment completion and was reassessed 4–6 weeks later. The response was clinically determined as complete response (CR), partial response (PR), stable disease (SD), and progressive disease (PD) by iRECIST [28].

Sample preparation

For the discovery phase, the serum specimens were obtained from 12 individual metastatic SCC and ADC patients. For the validation phase, an independent cohort including 15 patients was assessed individually by the chemical labeling quantitative method after IgG purification. Serial samples were collected before treatment (pre-trm) and after the first treatment cycle (trm), before the second cycle, from all patients with metastatic NSCLC treated with first-line ICIs. Blood samples were centrifuged for 10 min at 1200 *g* to obtain serum and stored at –80°C until use. The basic demographic and clinical characteristics of the participants are summarized in Table 1. Patients who were previously treated with special local therapies or who had incomplete clinical data were excluded.

Albumin depletion and in-gel digestion

Albumin Erasin Reagent (Sangon Biotech, Shanghai, China), which is specifically designed to effectively remove albumin from serum (https://www.sangon.com/), was applied according to the manufacturer's protocol. The albumin-depleted serum was separated by

Table 1. Clinical characteristics of patients with metastatic lung cancer receiving anti-PD-1/PD-L1 treatment

Patients and clinical characteristics	Responders (*n*=16)	Non-responders (*n*=11)
Median age at treatment start (years)	63 ± 3.87	61 ± 7.93
Sex		
Females, *n* (%)	1 (6.25)	1 (9.09)
Males, *n* (%)	15 (93.75)	10 (90.91)
Smoking, *n* (%)		
Never	2 (12.5)	1 (9.09)
Former/current	14 (87.5)	10 (90.91)
Pathology, *n* (%)		
Adenocarcinoma	9 (56.25)	7 (63.64)
Squamous	7 (43.75)	4 (36.36)
Clinical T stage, *n* (%)		
T1	1 (6.25)	0
T2	8 (50)	1 (9.09)
T3	3 (18.75)	4 (36.36)
T4	4 (25)	6 (54.55)
First-line therapy, *n* (%)		
Anti-PD-1	7 (43.75)	1 (9.09)
Anti-PD-L1	9 (56.25)	10 (90.91)
Treatment response, *n* (%)		
Complete response	1 (6.25)	0
Partial response	9 (56.25)	0
Stable disease	6 (37.5)	0
Progressive disease (no response)	0	11 (100)

10% SDS–PAGE. The protein bands were visualized with Coomassie blue and excised into small pieces. After reduction and alkylation, sequencing-grade modified trypsin (Promega, Madison, USA) was added and incubated at 37°C overnight. After lyophilization, the Glycopeptide Enrichment Kit was used according to the manufacturer's instructions (Novagen, Darmstadt, Germany).

IgG purification and in-solution digestion

Immunoglobulin G (IgG) was isolated from serum by using Protein G-agarose (Roche, Basel, Switzerland) in a spin column format according to the manufacturer's instructions. Serum diluted with binding/wash buffer (20 mM disodium hydrogen phosphate containing 0.15 M NaCl, pH 7.0) was loaded on the Protein G column. After a 3-h incubation, the column was washed with 30 mL binding/wash buffer to remove all non-IgG protein components and eluted with 10 mL of elution buffer (0.1 M glycine, pH 2.5). The collected fraction was neutralized with neutralizing buffer (1 M Tris-HCl, pH = 8.5) and ultrafiltered to concentrate the volume. The purified IgG and purification efficiency were confirmed by SDS-PAGE and quantified by the BCA method [29]. For protein digestion, concentrated IgG was diluted in 100 mM TEAB buffer (pH 8.0) at 0.5 mg/mL. After thermal denaturation, the reduction was performed at 56°C with 10 mM DTT for 1 h and then alkylated with 20 mM IAA for 45 min at room temperature. Then, the proteins were digested with trypsin (Promega, Madison, USA) overnight at 37°C.

Dimethylation and DMEN-amidation

After digestion, the solution containing 100 μg of IgG peptides was mixed with 17 μL of 4% formaldehyde solution (HCHO_light or DCDO_heavy) and 17 μL of 0.6 M sodium cyanoborohydride solution ($NaBH_3CN$_light or $NaBD_3CN$_heavy). The mixture was incubated at 37°C for 2 h. After termination of the reaction, the dimethyl-labeled peptides were desalted with a C18 SPE cartridge and then lyophilized under vacuum. The DMEN-amidation condition was described previously [29]. The derivatized N-glycopeptides were enriched using an in-house ZIC-HILIC microcolumn and subsequently dried by vacuum centrifugation for further analysis [30].

LC-MS/MS analysis

For the glycopeptide derived from albumin-erased serum, Nano-Liquid Chromatography Tandem MS was used as previously described [31,32]. For the glycopeptide derived from IgG samples, the mixture was analyzed on an Orbitrap Fusion Tribrid (Thermo Fisher Scientific, Waltham, USA) connected to an EASYnLC 1000 system (Thermo Fisher Scientific). The obtained IgG glycopeptide (approximately 3 μg) was dissolved in Solvent A to 16 μL, and 4 μL was loaded onto the analytical column (Dionex Acclaim PepMap C18, 75 μm × 50 cm) with a flow rate of 200 nL/min. The gradient was totally 60 min: 2%–40% B from 0 to 45 min, 40%–60% from 46 min to 54 min, followed by an increase to 100% in 1 min, and 100% B for the last 5 min (Solvent A: water containing 0.1% formic acid; Solvent B: acetonitrile containing 0.1% formic acid). The MS parameters were set as follows. MS1: scan range (m/z) = 350–2000; resolution = 120 k; AGC target = 1,000,000; maximum injection time = 50 ms; dynamic exclusion after n times, $n = 1$; dynamic exclusion duration = 12 s; each selected precursor was subject to one HCD-MS/MS and one ETD-MS/MS. MS/MS: isolation window = 2; detector type = Orbitrap; resolution = 15 k; AGC target = 200,000; maximum injection time = 150 ms; HCD collision energy = 30%; stepped collision mode on; energy difference of ± 10%.

Glycoproteomic analysis

For label-free data, the intact glycopeptides were identified by pGlyco (http://pfind.ict.ac.cn/software/pGlyco/index.html) and quantified by pQuant with parameters described previously [31,33,34]. For chemical labeling data, the glycopeptides were identified and quantified by the combination of Byonic and Byologic software (Protein Metrics, San Carlos, USA) with parameters described earlier [30]. Thus, the quantitative results among the samples were compared automatically [35]. XCalibur 3.0 was used for manual validation [36]. The mass spectrometry proteomics data have been deposited in the ProteomeXchange Consortium (http://proteomecentral.proteomexchange.org) via the iProX partner repository [37,38] with the dataset identifier PXD039141.

Statistical analysis

Graphs were generated with GraphPad Prism 8.0 (GraphPad Software Inc, La Jolla, USA) and Hiplot (https://hiplot.com.cn) [39], which are powerful web platforms for scientific data visualization. Statistical comparisons were calculated using t-test. P values less than 0.05 were considered statistically significant, and all reported P values were two-tailed.

Results

Serum samples and label-free quantification

To detect changes in the serum glycoproteome attributable to treatment, 12 patients with metastatic SCC and ADC undergoing first-line anti-PD-1/PD-L1 treatment were enrolled (Figure 1). Responders to anti-PD-1/PD-L1 treatment, that is, patients with CR, PR, or SD, and non-responders, patients with PD. Human serum was collected before and after the treatment of anti-PD-1/PD-L1 immunotherapy (pre-trm and trm).

Label-free quantitation method was utilized to perform comparisons associated with anti-PD-1/PD-L1 treatment (Figure 2A). In order to reduce the interference from the enrichment process, an equal volume of serum was acquired individually to remove albumin. A representative gel image is shown in Supplementary Figure S1. By using the commercial Glycopeptide Enrichment Kit, N-glycopeptides in albumin-free serum were investigated by nano-LC-HCD-MS/MS. After each serum experiment, the blank was run to ensure no carry-over.

To simplify the glycan annotation, a four-digit nomenclature in HNSF order was used (H, Hexose; N, N-acetylhexosamine; S, Sialic acid; F, Fucose). Totally, 2036 N-glycopeptides in albumin-free serum were detected (Supplementary Table S1) in lung cancer patients and assigned to 321 glycoproteins. Approximately 81.31% of N-glycoproteins in lung cancer patients were identified with one *in vivo* N-glycosylation site, 10.28% with two N-glycosites, and 3.11% with more than three N-glycosites (Figure 2B). Comparing the distribution of N-glycan compositions, H5N4S2 represented biantennary fully sialylated oligosaccharide, the most common composition in the detection (Figure 2C).

Glycosylation changes associated with anti-PD-1/PD-L1 treatment

At the very beginning, we explored the overall changes in serum glycopeptides during anti-PD-1/PD-L1 treatment, regardless of treatment response. In patients treated with anti-PD-1/PD-L1 inhibitors,

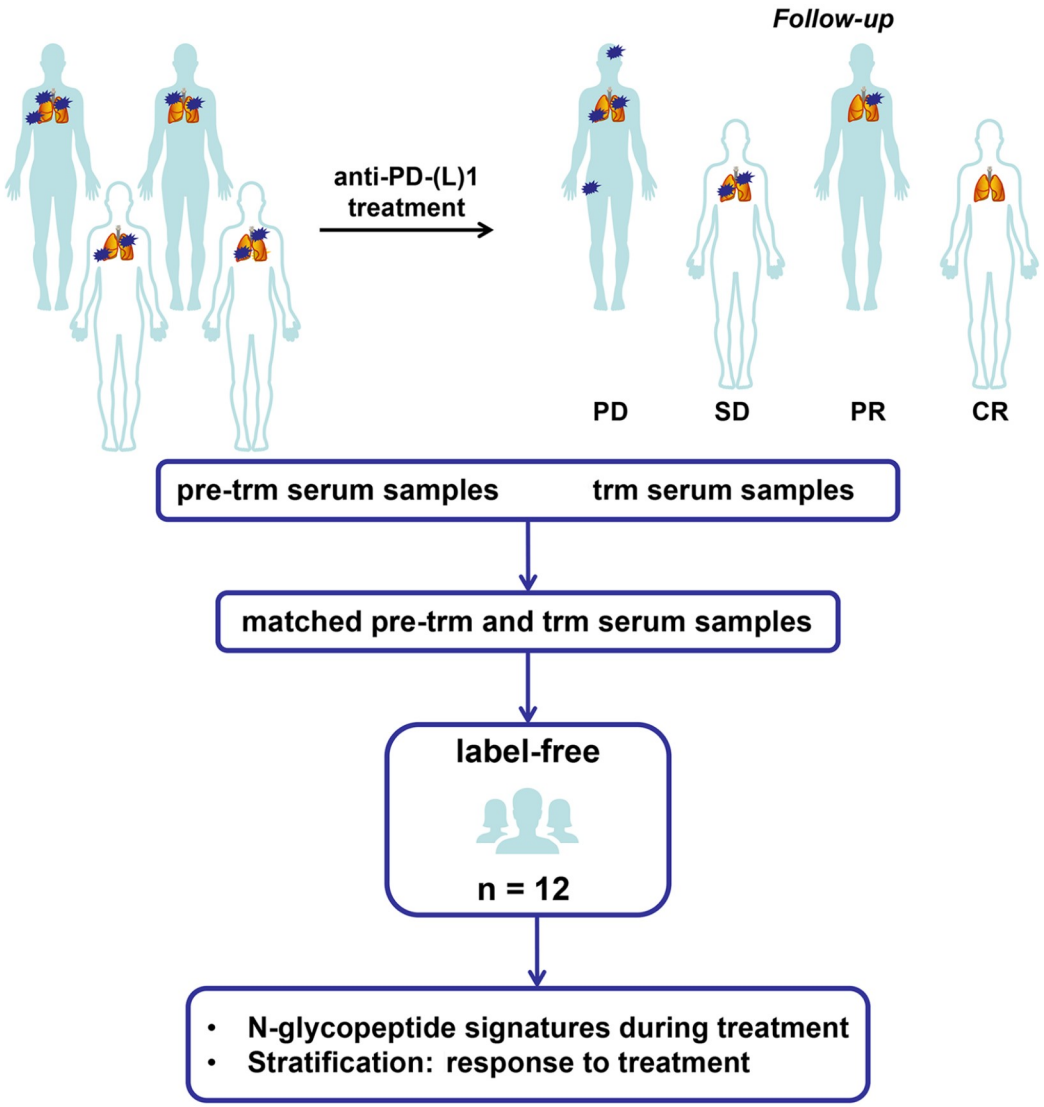


Figure 1. Collection of serum samples during anti-PD-1/PD-L1 immunotherapy in the discovery cohort Serum samples from patients with advanced lung cancer undergoing anti-PD-1/PD-L1 immunotherapy were obtained before the initiation of treatment (pre-trm) and during the course of therapy, specifically after the first treatment cycle (trm). The samples were analyzed to identify changes in glyco-signatures associated with the response to immunotherapy.

337 N-glycopeptides passed stringent filtering criteria as described [31,32], and quantitative information was obtained (Supplementary Table S2). Among them, 27 N-glycopeptides had significant changes in serum levels during treatment according to LC-HCD-MS/MS data ($P < 0.05$; Figure 3A), with CERU_N397 (H6N4S1F1) and IGHG4_N177 (H3N4) having the largest increase ($P = 0.0095$ and $P = 0.0083$, respectively). In addition, IGHM_N209 (H5N5S1F1) had the largest decrease as compared with pre-treatment ($P = 0.0244$).

To explore the biological functions of the glycoproteins with tendency, gene ontology (GO) enrichment analysis was performed. The majority of the glycoproteins altered during anti-PD-1/PD-L1 treatment were significantly linked to negative regulation of endopeptidase activity, complement activation, platelet degranulation, and innate immune response (Figure 3B). In addition, endopeptidase inhibitor activity, heparin binding and complement binding were significantly enriched in the GO-MF category (Figure 3C). Most glycoproteins were selectively enriched for GO cellular component (CC) categories linked to blood microparticles, extracellular regions, and extracellular exosomes (Figure 3D).

N-glycopeptide signatures in anti-PD-1/PD-L1 responders

Stratifying the patients according to response showed that 24 N-glycopeptides had altered serum levels during treatment in the subgroup of anti-PD-1/PD-L1 responders according to the label-free data ($P < 0.05$), with IGHG4_N177 (H3N4) showing the largest increase (Figure 4A and Supplementary Figure S2). However, only one glycopeptide showed a significant change during treatment among the anti-PD-1/PD-L1 non-responders, implying there were quite differences in protein glycosylation between responders and non-responders (Figure 4A and Supplementary Table S3). Similar to the global analysis, glycoproteins with characteristic changes in anti-PD-1/PD-L1 responders during treatment were involved in a series of processes, such as complement activation, innate immune response

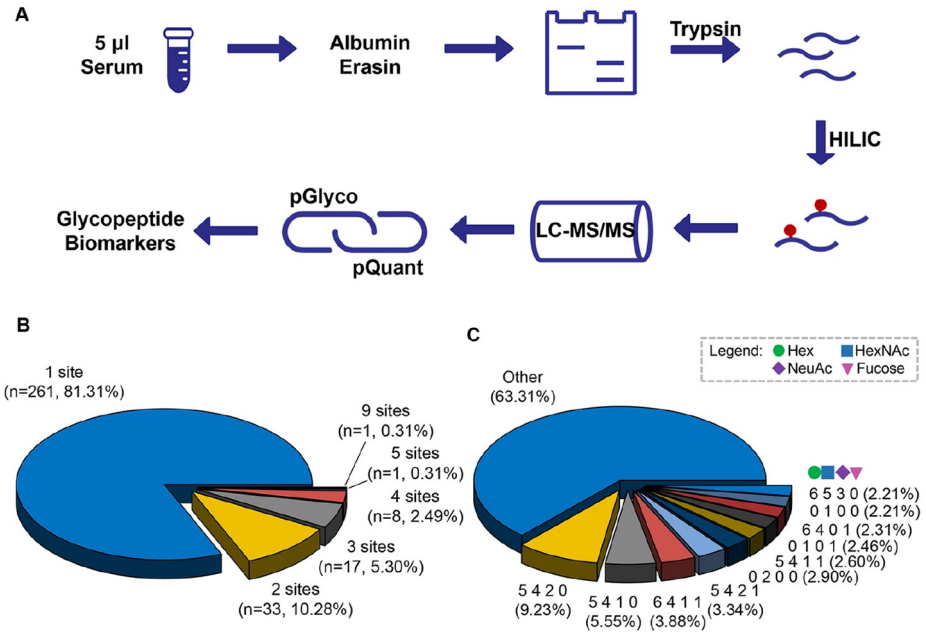


Figure 2. Label-free quantitation methodology for serum glycopeptide analysis (A) Workflow for label-free quantification of N-glycopeptides in serum samples from patients receiving anti-PD-1/PD-L1 immunotherapy. The process included serum collection, albumin depletion, in-gel digestion, glycopeptide enrichment, and mass spectrometry analysis. (B) Pie chart depicting the distribution of proteins with single or multiple N-glycosylation sites in the serum samples. (C) Pie chart displaying the frequency of various N-glycan compositions identified in serum, with the most common composition indicated.

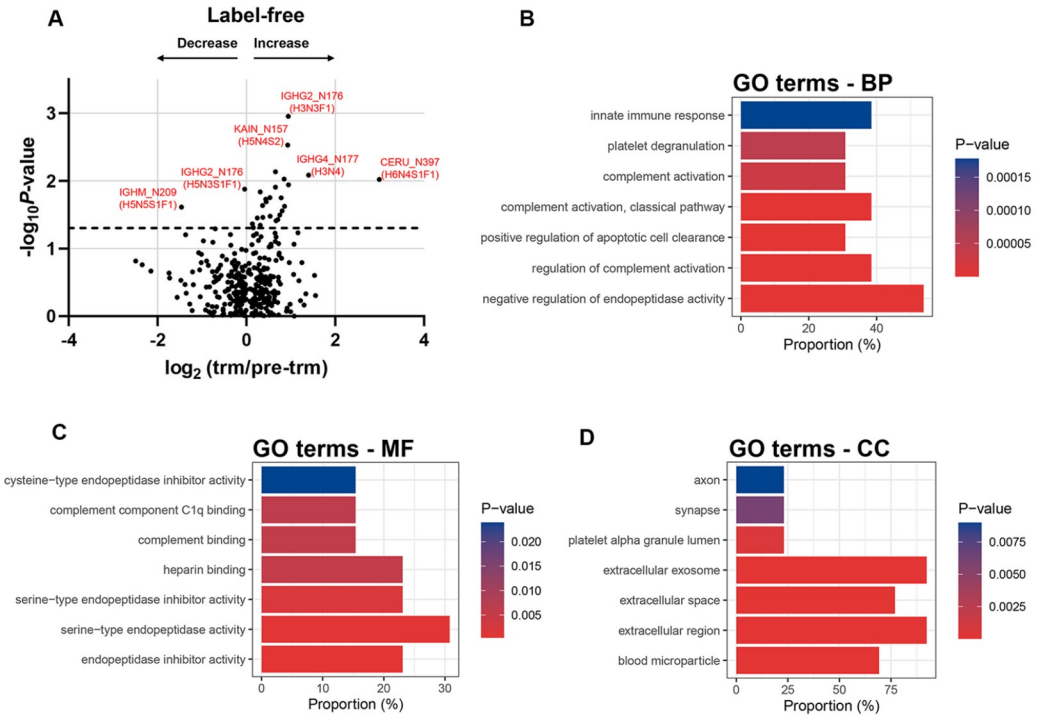


Figure 3. Glycosylation changes associated with anti-PD-1/PD-L1 treatment (A) Volcano plots on comparing trm with pre-trm glycopeptides in serum of metastatic NSCLC patients who were treated with anti-PD-1/PD-L1 inhibitors (two-sided paired *t* test). Glycopeptides above the dashed line indicate a *P*-value that is less than 0.05. (B–D) GO biological process (BP), molecular function (MF), and cellular component (CC) categories enriched in the anti-PD-1/PD-L1 treatment cohort. GO, gene ontology; pre-trm, pre-treatment; trm, after the first treatment cycle.

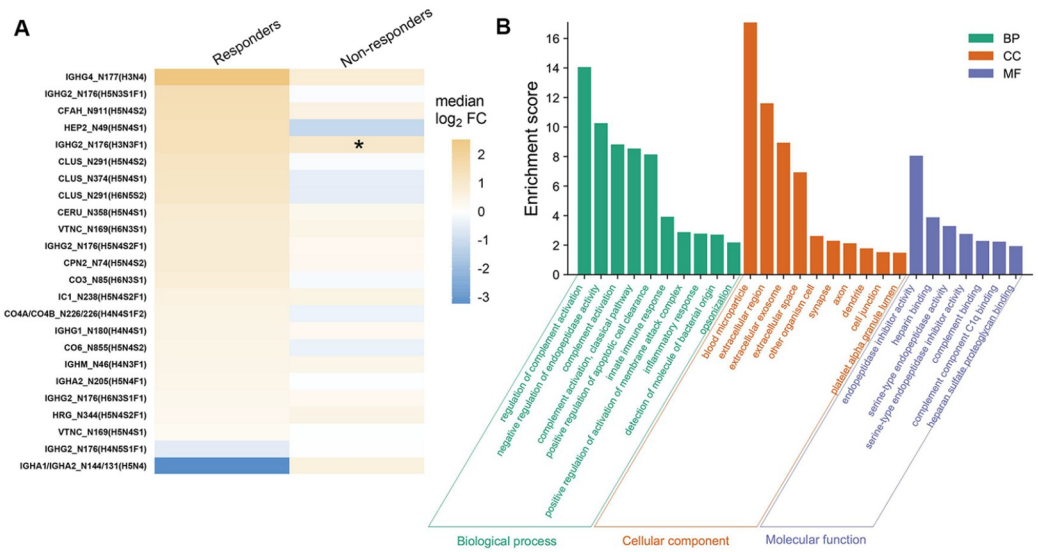


Figure 4. N-glycopeptide signatures in anti-PD-1/PD-L1 responders (A) In the stratification analyses, heat map displayed relative abundance of differentially expressed glycopeptides in serum during treatment in the subgroup of anti-PD-1/PD-L1 responders, with corresponding changes during treatment in anti-PD-1/PD-L1 non-responders (two-sided paired *t* test). The glycopeptide that had a statistically significant change in non-responders was marked with an * ($P < 0.05$). (B) GO enrichment analysis of the glycoproteins with a change in serum levels during treatment in the subgroup of anti-PD-1/PD-L1 responders.

and inflammation response, according to their GO terms (Figure 4B). The responder and non-responder groups also differed in N-glycopeptide levels before drug application (Supplementary Figure S3).

High-throughput analysis of IgG glycopeptides by chemical labeling

Through a global analysis of the serum glycoproteome, 24 N-glycopeptides were screened out to have significant changes in serum of responders to anti-PD-1/PD-L1 blockade, among which 7 glycopeptides belonged to the IgG family, accounting for the absolute majority, suggesting that the serum IgG glycosylation level might reflect the effectiveness of tumor immunotherapy (Figure 4A). Considering the high frequency of variation in IGHG (IgG) intact glycopeptides observed in anti-PD-1/PD-L1 responders, large-scale site-specific profiling of IgG glycosylation is recommended for further validation. Hence, we performed IgG purification and chemical labeling to achieve comprehensive N-glycosylation analysis in all subclasses of IgG (Figure 5A and Supplementary Figure S4A). Finally, a total of 209 IgG N-glycopeptides were identified after DMEN-labeling and HILIC enrichment (Supplementary Table S4). Among them, 26 IgG N-glycopeptides met stringent filtering criteria (Supplementary Figure S4B) and provided quantitative information (Supplementary Table S5).

Based on labeling quantification, there was a significant increase in the serum level of IGHG4_N177 (H3N4) during treatment in anti-PD-1/PD-L1 responders compared with anti-PD-1/PD-L1 non-responders ($P < 0.05$, Figure 5B). In addition, the expression of another glycopeptide, IGHG3_N227 (H3N4F1), significantly increased during treatment in the anti-PD-1/PD-L1 non-responders, as compared with the responders in the validation cohort ($P < 0.05$, Figure 5C). Representative MS^1 spectra and MS^2 annotations of IGHG4_N177 (H3N4) and IGHG3_N227 (H3N4F1) is shown in Figure 6.

Discussion

Immune checkpoint inhibitors are improving the prognosis of patients with human cancers [40]. In particular, checkpoint inhibitors targeting PD-1 and PD-L1 have shown unprecedented curative effects in a variety of tumors, including melanoma, renal cell carcinoma and non-small cell lung cancer [41]. However, the therapy with biologics is cost-intensive and have limited response rates, which means that efforts are urgently needed to reduce the burden of medical expenses [42]. With the development of personalized medicine, the integration of multi-omics technology will promote comprehensive disclosure of dynamic changes during treatment [43]. Furthermore, the dynamic changes in the treatment process may be used to assess response before radiological changes are apparent, and these changes may also help us delineate mechanisms that underpin both response and resistance to ICIs [13].

Multiple sources reported that the alterations in glycosylation are common in cancer and are thought to provide novel typical features and therapeutic targets [18]. Intact glycopeptide analysis including glycosylation sites and site-specific glycans is essential to understand the biological significance of glycosylation [32]. Currently, a total of 2036 glycopeptides were identified, and 337 glycopeptides were quantified, which is the first comprehensive study on serum glycoproteome of patients with advanced SCC and ADC receiving anti-PD-1/PD-L1 treatment. Although the sample size was limited, this study was elaborately designed with an independent discovery and validation cohort. Sufficient independent repetition and standardized procedures, combined with robust chemical labeling quantitative analysis methods, enable us to accurately locate the glycosylation changes of serum proteins specific to anti-PD-1/PD-L1 treatment, ensuring the quantitative reproducibility of the entire strategy, which is key for biomarker screening. According to the short-term response of patients, the stratified analysis provides us with unique insight into the changes of circulating glycoproteins during treatment. It is worth mentioning that complement activation is an example of the common process induced by anti-PD-1/PD-L1 treatment [44,45], which is also one of the biological processes associated with a high proportion of glycoprotein changes in anti-PD-1/PD-L1 responders.

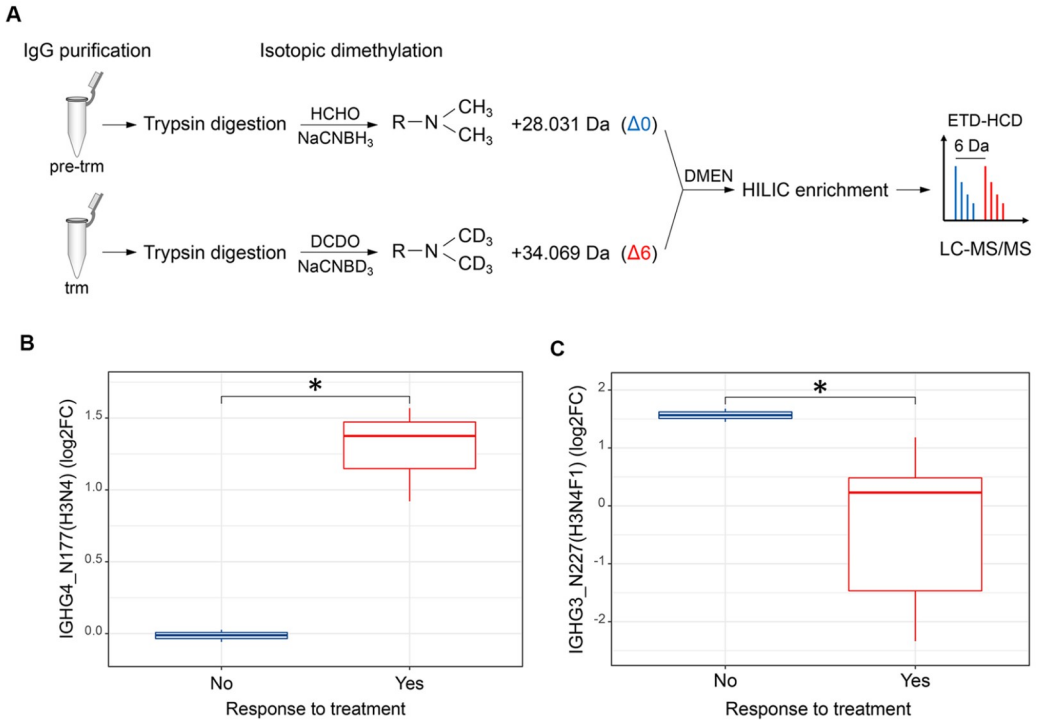


Figure 5. High-throughput analysis of IgG glycopeptides by chemical labeling (A) Chemical labeling for fine mapping of IgG N-glycopeptides during anti-PD-1/PD-L1 treatment in the validation cohort. IGHG4_N177 (H3N4) (B) and IGHG3_N227 (H3N4F1) (C) represent significant differences between anti-PD-1/PD-L1 responders and non-responders. *$P < 0.05$.

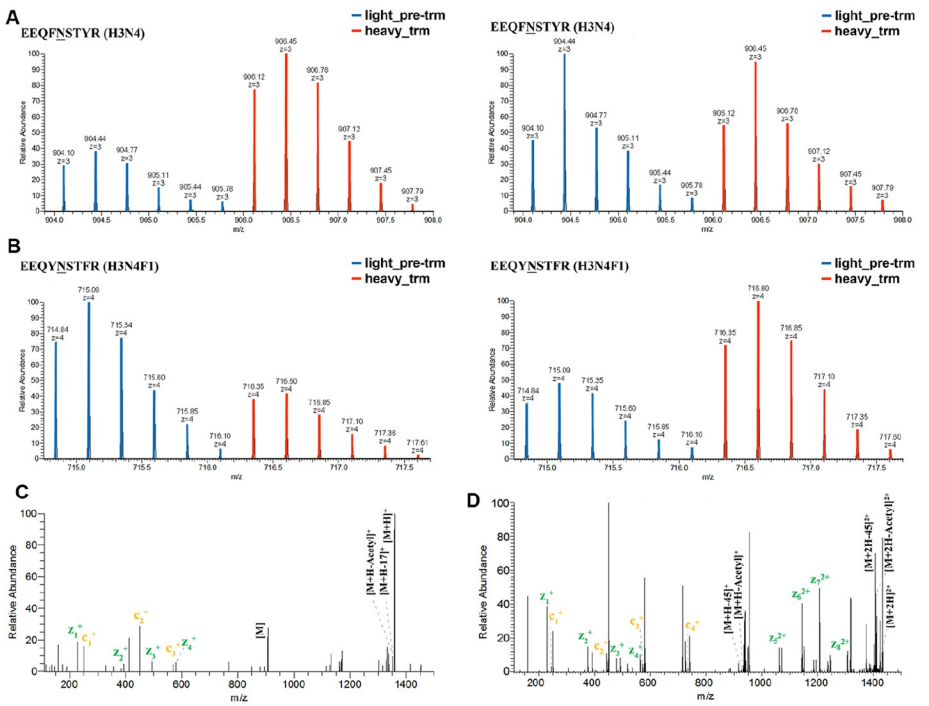


Figure 6. Representative MS¹ spectra and MS² annotations (A) Representative mass spectrum of IGHG4_N177 (H3N4) in anti-PD-1/PD-L1 responders (left) and non-responders (right). pQuant reported that the trm/pre-trm ratio was 2.59 and 0.99, respectively. (B) Representative mass spectrum of IGHG3_N227 (H3N4F1) in anti-PD-1/PD-L1 responders (left) and non-responders (right). pQuant reported that the trm/pre-trm ratio was 0.36 and 2.84, respectively. The ETD MS/MS spectra of the N-glycopeptide IGHG4_N177 (H3N4) (C) and IGHG3_N227 (H3N4F1) (D).

IgG is the most abundant glycoprotein in serum, with a total molecular weight of about 150 kDa, which is an important part of body protective immunity [46]. According to the amino acid sequence of the heavy chain constant region, IgGs can be divided into four subclasses: IgG1, IgG2 and IgG3 and IgG4 [47]. IgG subclasses activate the complement system through a classical pathway with different abilities and bind to specific receptors on macrophages and neutrophils [48]. Changes in the glycosylation profiles of serum IgG affect immunoglobulin function and have been described in some physiological processes, such as pregnancy or aging [49,50], as well as in many pathological conditions, such as chronic obstructive pulmonary disease (COPD), ischemic stroke or asthma [51–53]. Our study highlights that after anti-PD-1/PD-L1 immunotherapy, there is an upregulation of IGHG4_N177 (H3N4) in the serum of lung cancer patients, which seems to point to unique immunological processes [54]. Interestingly, recent studies have shown that IgG4 autoantibodies are able to activate the lectin complement pathway and induce cell injury in a glycosylation-dependent manner [55]. As we known, IgG N-glycosylation undergoes minimal changes in homeostasis, while extreme changes may occur in inflammation or disease status [56]. Notably, the structure and effector function of IgG are regulated by N-glycosylation. Specific IgG glycosylation can convert pro-inflammatory responses to anti-inflammatory activities, mediating two completely opposite immunological effects [57]. The two IgG glycopeptides discussed in this study exhibit different trends during the treatment process and may have different functions in antitumor immunity. In theory, glycosylation of IgG affects antibody half-life, isoelectric point, binding affinity, secondary structure, and thermal stability, then affects its affinity for the antigen, the function of the antibody itself, and receptor-mediated signal transduction [58]. In particular, research has shown that core fucose could affect the binding of IgG antibody to the endogenous ligand protein Dectin-1, mediating the attenuation of the antibody-dependent cellular cytotoxicity of IgG antibodies [59]. More efforts should be made to study the function of immunoglobulin site-specific glycan in tumor immunity, especially from the perspective of protein-protein interactions. Other differentially expressed glycoproteins should be further studied by other glycoproteomics methods.

In summary, MS-based quantification methods combining labeling and label-free were used to define glyco-signatures in patients with advanced SCC and ADC receiving anti-PD-1/PD-L1 treatment. The results suggested that site-specific glycoforms on serum IgG may be a useful *in vitro* complementary test to enhance proper clinical management. Multicenter studies with large samples are needed to evaluate the practicability of the results and to translate them into clinical practice.

Supplementary Data

Supplementary data is available at *Acta Biochimica et Biophysica Sinica* online.

Funding

This work was supported by the grants from the National Key Research and Development Program of China (No. 2022YFC3400800), the National Natural Science Foundation of China (Nos. 21974025 and 82121004), the Shanghai Projects (Nos. 22142202400 and 22DZ2291700), and the Greater Bay Area Institute of Precision Medicine (No. IPM2021C005).

Conflict of Interest

The authors declare that they have no conflict of interest.

References

1. Thai AA, Solomon BJ, Sequist L, Gainor JF, Heist RS. Lung cancer. *Lancet* 2021, 398: 535–554
2. Goldberg SB, Herbst RS. The end of the beginning: progress and next steps in KRAS-mutant non-small-cell lung cancer. *Lancet* 2023, 401: 706–707
3. Sung H, Ferlay J, Siegel RL, Laversanne M, Soerjomataram I, Jemal A, Bray F. Global cancer statistics 2020: globocan estimates of incidence and mortality worldwide for 36 cancers in 185 countries. *CA Canc J Clin* 2021, 71: 209–249
4. Petty WJ, Paz-Ares L. Emerging strategies for the treatment of small cell lung cancer. *JAMA Oncol* 2023, 9: 419–429
5. Sholl LM. Biomarkers of response to checkpoint inhibitors beyond PD-L1 in lung cancer. *Modern Pathol* 2022, 35: 66–74
6. Tang S, Qin C, Hu H, Liu T, He Y, Guo H, Yan H, *et al.* Immune checkpoint inhibitors in non-small cell lung cancer: progress, challenges, and prospects. *Cells* 2022, 11: 320
7. Gainor JF. Adjuvant PD-L1 blockade in non-small-cell lung cancer. *Lancet* 2021, 398: 1281–1283
8. Topalian SL, Hodi FS, Brahmer JR, Gettinger SN, Smith DC, McDermott DF, Powderly JD, *et al.* Safety, activity, and immune correlates of anti-PD-1 antibody in cancer. *N Engl J Med* 2012, 366: 2443–2454
9. Jiang J, Jin Z, Zhang Y, Peng L, Zhang Y, Zhu Z, Wang Y, *et al.* Robust prediction of immune checkpoint inhibition therapy for non-small cell lung cancer. *Front Immunol* 2021, 12: 646874
10. Tang Q, Chen Y, Li X, Long S, Shi Y, Yu Y, Wu W, *et al.* The role of PD-1/PD-L1 and application of immune-checkpoint inhibitors in human cancers. *Front Immunol* 2022, 13: 964442
11. Terranova-Barberio M, Pawlowska N, Dhawan M, Moasser M, Chien AJ, Melisko ME, Rugo H, *et al.* Exhausted T cell signature predicts immunotherapy response in ER-positive breast cancer. *Nat Commun* 2020, 11: 3584
12. Newton HS, Gawali VS, Chimote AA, Lehn MA, Palackdharry SM, Hinrichs BH, Jandarov R, *et al.* PD1 blockade enhances K^+ channel activity, Ca^{2+} signaling, and migratory ability in cytotoxic T lymphocytes of patients with head and neck cancer. *J Immunother Canc* 2020, 8: e000844
13. Lavoie JM, Baichoo P, Chavez E, Nappi L, Khalaf D, Kollmannsberger CK, Chi KN, *et al.* Comprehensive immune profiling of patients with advanced urothelial or renal cell carcinoma receiving immune checkpoint blockade. *Front Oncol* 2022, 12: 973402
14. Hossain SM, Gimenez G, Stockwell PA, Tsai P, Print CG, Rys J, Cybulska-Stopa B, *et al.* Innate immune checkpoint inhibitor resistance is associated with melanoma sub-types exhibiting invasive and de-differentiated gene expression signatures. *Front Immunol* 2022, 13: 955063
15. Wu Z, Zhang S, Li L, Huang Z, Huang D, Hu Y. The gut microbiota modulates responses to anti-PD-1 and chemotherapy combination therapy and related adverse events in patients with advanced solid tumors. *Front Oncol* 2022, 12: 887383
16. Schjoldager KT, Narimatsu Y, Joshi HJ, Clausen H. Global view of human protein glycosylation pathways and functions. *Nat Rev Mol Cell Biol* 2020, 21: 729–749
17. Ren X, Wu L, Zhang L, Liu Y, Wang G, Lu H. Discovery of age-related early-stage glycated proteins based on deep quantitative serum glycated proteome analysis. *Acta Biochim Biophys Sin* 2023, 55: 1659–1667
18. Wang Y, Chen H. Protein glycosylation alterations in hepatocellular carcinoma: Function and clinical implications. *Oncogene* 2023, 42: 1970–1979
19. Chang X, Obianwuna UE, Wang J, Zhang H, Qi G, Qiu K, Wu S. Glycosylated

proteins with abnormal glycosylation changes are potential biomarkers for early diagnosis of breast cancer. *Int J Biol Macromol* 2023, 236: 123855
20. Oh MJ, Lee SH, Kim U, An HJ. In-depth investigation of altered glycosylation in human haptoglobin associated cancer by mass spectrometry. *Mass Spectrometry Rev* 2023, 42: 496–518
21. Hatakeyama S, Yoneyama T, Tobisawa Y, Yamamoto H, Ohyama C. Narrative review of urinary glycan biomarkers in prostate cancer. *Transl Androl Urol* 2021, 10: 1850–1864
22. Chau TH, Chernykh A, Kawahara R, Thaysen-Andersen M. Critical considerations in N-glycoproteomics. *Curr Opin Chem Biol* 2023, 73: 102272
23. Haslund-Gourley BS, Wigdahl B, Comunale MA. IgG N-glycan signatures as potential diagnostic and prognostic biomarkers. *Diagnostics* 2023, 13: 1016
24. Delafield DG, Li L. Recent advances in analytical approaches for glycan and glycopeptide quantitation. *Mol Cell Proteomics* 2021, 20: 100054
25. Cao W, Liu M, Kong S, Wu M, Zhang Y, Yang P. Recent advances in software tools for more generic and precise intact glycopeptide analysis. *Mol Cell Proteomics* 2021, 20: 100060
26. Cao X, Shao Y, Meng P, Cao Z, Yan G, Yao J, Zhou X, ***et al.*** Nascent proteome and glycoproteome reveal the inhibition role of ALG1 in hepatocellular carcinoma cell migration. *Phenomics* 2022, 2: 230–241
27. Ettinger DS, Wood DE, Aisner DL, Akerley W, Bauman JR, Bharat A, Bruno DS, ***et al.*** NCCN guidelines insights: non–small cell lung cancer, version 2.2021. *J Natl Compr Canc Netw* 2021, 19: 254–266
28. Ferté C, Marabelle A. iRECIST: a clarification of tumour response assessment in the immunotherapy era. *Eur J Canc* 2017, 77: 165–167
29. Yang L, Sun Z, Zhang L, Cai Y, Peng Y, Cao T, Zhang Y, ***et al.*** Chemical labeling for fine mapping of IgG N-glycosylation by ETD-MS. *Chem Sci* 2019, 10: 9302–9307
30. Sun Z, Ji G, Wang G, Wei L, Zhang Y, Lu H. One step carboxyl group isotopic labeling for quantitative analysis of intact *N*-glycopeptides by mass spectrometry. *Chem Commun* 2021, 57: 4154–4157
31. Zhang S, Cao X, Liu C, Li W, Zeng W, Li B, Chi H, ***et al.*** N-glycopeptide signatures of IgA_2 in serum from patients with hepatitis B virus-related liver diseases. *Mol Cell Proteomics* 2019, 18: 2262–2272
32. Cao X, Cao Z, Shao Y, Liu C, Yan G, Meng X, Zhang L, ***et al.*** Analysis of serum paraoxonase 1 using mass spectrometry and lectin immunoassay in patients with alpha-fetoprotein negative hepatocellular carcinoma. *Front Oncol* 2021, 11: 651421
33. Kong S, Gong P, Zeng WF, Jiang B, Hou X, Zhang Y, Zhao H, ***et al.*** pGlycoQuant with a deep residual network for quantitative glycoproteomics at intact glycopeptide level. *Nat Commun* 2022, 13: 7539
34. Liu C, Song CQ, Yuan ZF, Fu Y, Chi H, Wang LH, Fan SB, ***et al.*** pQuant improves quantitation by keeping out interfering signals and evaluating the accuracy of calculated ratios. *Anal Chem* 2014, 86: 5286–5294
35. Zhu J, Huang J, Zhang J, Chen Z, Lin Y, Grigorean G, Li L, ***et al.*** Glycopeptide biomarkers in serum haptoglobin for hepatocellular carcinoma detection in patients with nonalcoholic steatohepatitis. *J Proteome Res* 2020, 19: 3452–3466
36. Li Y, Qu J, Lin Y, Lu G, You Y, Jiang G, Wu Y. Visible post-data analysis protocol for natural mycotoxin production. *J Agric Food Chem* 2020, 68: 9603–9611
37. Ma J, Chen T, Wu S, Yang C, Bai M, Shu K, Li K, ***et al.*** iProX: an integrated proteome resource. *Nucleic Acids Res* 2019, 47: D1211–D1217
38. Chen T, Ma J, Liu Y, Chen Z, Xiao N, Lu Y, Fu Y, ***et al.*** iProX in 2021: connecting proteomics data sharing with big data. *Nucleic Acids Res* 2022, 50: D1522–D1527
39. Li J, Miao B, Wang S, Dong W, Xu H, Si C, Wang W, ***et al.*** Hiplot: a comprehensive and easy-to-use web service for boosting publication-ready biomedical data visualization. *Brief Bioinform* 2022, 23: bbac261
40. Hollern DP, Xu N, Thennavan A, Glodowski C, Garcia-Recio S, Mott KR, He X, ***et al.*** B cells and T follicular helper cells mediate response to checkpoint inhibitors in high mutation burden mouse models of breast cancer. *Cell* 2019, 179: 1191–1206.e21
41. O'Donnell JS, Long GV, Scolyer RA, Teng MWL, Smyth MJ. Resistance to PD1/PDL1 checkpoint inhibition. *Canc Treat Rev* 2017, 52: 71–81
42. Perdyan A, Sobocki BK, Balihodzic A, Dąbrowska A, Kacperczyk J, Rutkowski J. The effectiveness of cancer immune checkpoint inhibitor retreatment and rechallenge—a systematic review. *Cancers* 2023, 15: 3490
43. Bulgarelli J, Pignatta S, Petrini M, Ridolfi L. The renewal of cancer immunotherapy. *Vaccines* 2023, 11: 592
44. Magrini E, Minute L, Dambra M, Garlanda C. Complement activation in cancer: effects on tumor-associated myeloid cells and immunosuppression. *Semin Immunol* 2022, 60: 101642
45. Pio R, Ajona D, Ortiz-Espinosa S, Mantovani A, Lambris JD. Complementing the cancer-immunity cycle. *Front Immunol* 2019, 10: 774
46. Arnold JN, Wormald MR, Sim RB, Rudd PM, Dwek RA. The impact of glycosylation on the biological function and structure of human immunoglobulins. *Annu Rev Immunol* 2007, 25: 21–50
47. Jefferis R. Glycosylation as a strategy to improve antibody-based therapeutics. *Nat Rev Drug Discov* 2009, 8: 226–234
48. Shkunnikova S, Mijakovac A, Sironic L, Hanic M, Lauc G, Kavur MM. IgG glycans in health and disease: prediction, intervention, prognosis, and therapy. *Biotechnol Adv* 2023, 67: 108169
49. Bondt A, Rombouts Y, Selman MHJ, Hensbergen PJ, Reiding KR, Hazes JMW, Dolhain RJEM, ***et al.*** Immunoglobulin G (IgG) fab glycosylation analysis using a new mass spectrometric high-throughput profiling method reveals pregnancy-associated changes. *Mol Cell Proteomics* 2014, 13: 3029–3039
50. Gudelj I, Lauc G, Pezer M. Immunoglobulin G glycosylation in aging and diseases. *Cell Immunol* 2018, 333: 65–79
51. Komaromy A, Reider B, Jarvas G, Guttman A. Glycoprotein biomarkers and analysis in chronic obstructive pulmonary disease and lung cancer with special focus on serum immunoglobulin G. *Clinica Chim Acta* 2020, 506: 204–213
52. Wang B, Gao L, Zhang J, Meng X, Xu X, Hou H, Xing W, ***et al.*** Unravelling the genetic causality of immunoglobulin G N-glycans in ischemic stroke. *Glycoconj J* 2023, 40: 413–420
53. Sodemann EB, Dähling S, Klopfleisch R, Boiarina E, Cataldo D, Alhasan MM, Yildirim AÖ, ***et al.*** Maternal asthma is associated with persistent changes in allergic offspring antibody glycosylation. *Clin Exp Allergy* 2020, 50: 520–531
54. Yang S, Cui M, Liu Q, Liao Q. Glycosylation of immunoglobin G in tumors: function, regulation and clinical implications. *Canc Lett* 2022, 549: 215902
55. Haddad G, Lorenzen JM, Ma H, de Haan N, Seeger H, Zaghrini C, Brandt S, ***et al.*** Altered glycosylation of IgG4 promotes lectin complement pathway activation in anti-PLA2R1–associated membranous nephropathy. *J Clin Invest* 2021, 131: e140453
56. Trzos S, Link-Lenczowski P, Pocheć E. The role of N-glycosylation in B-cell biology and IgG activity. The aspects of autoimmunity and anti-inflammatory therapy. *Front Immunol* 2023, 14: 1188838
57. Liu S, Liu X. IgG N-glycans. *Adv Clin Chem* 2021, 105: 1–47
58. Ding K, Han L, Zong H, Chen J, Zhang B, Zhu J. Production process reproducibility and product quality consistency of transient gene expression in HEK293 cells with anti-PD1 antibody as the model protein. *Appl Microbiol Biotechnol* 2017, 101: 1889–1898
59. Manabe Y, Marchetti R, Takakura Y, Nagasaki M, Nihei W, Takebe T, Tanaka K, ***et al.*** The core fucose on an IgG antibody is an endogenous ligand of Dectin-1. *Angew Chem Int Ed* 2019, 58: 18697–18702